

SCIENTIFIC REPORTS

OPEN

Unexplored photoluminescence from bulk and mechanically exfoliated few layers of Bi_2Te_3

Bipin Kumar Gupta¹, Rabia Sultana^{1,2}, Satbir Singh^{1,2}, Vijeta Singh^{1,2}, Geet Awana^{1,3}, Anurag Gupta¹, Bahadur Singh⁴, A. K. Srivastava¹, O. N. Srivastava⁵, S. Auluck¹ & V. P. S. Awana¹

We report the exotic photoluminescence (PL) behaviour of 3D topological insulator Bi_2Te_3 single crystals grown by customized self-flux method and mechanically exfoliated few layers (18 ± 2 nm)/thin flakes obtained by standard scotch tape method from as grown Bi_2Te_3 crystals. The experimental PL studies on bulk single crystal and mechanically exfoliated few layers of Bi_2Te_3 evidenced a broad red emission in the visible region from 600–690 nm upon 375 nm excitation wavelength corresponding to optical band gap of 2 eV. These findings are in good agreement with our theoretical results obtained using the *ab initio* density functional theory framework. Interestingly, the observed optical band gap is several times larger than the known electronic band gap of ~ 0.15 eV. The experimentally observed 2 eV optical band gap in the visible region for bulk as well as for mechanically exfoliated few layers Bi_2Te_3 single crystals clearly rules out the quantum confinement effects in the investigated samples which are well known in the 2D systems like MoS_2 , WS_2 , WSe_2 , and MoSe_2 for 1–3 layers.

Recently, topological insulators (TIs) have gained a huge attention among condensed matter physicists credited to their striking multifunctional properties^{1,2}. The most famous examples of 3D TIs are Bi_2Te_3 , Bi_2Se_3 and Sb_2Te_3 . These materials act as prototypical TIs because of their large intrinsic electronic band gap with a single Dirac-cone-like topologically protected metallic surface state inside the bulk energy gap. The interesting duality of this quantum materials viz., insulating from interior and conducting at the surface gives rise to many interesting properties with novel physics and potential for applications. Additionally due to the spin-momentum locked Dirac-cone surface states, TIs exhibit large un-saturating magneto resistance^{3–5} and are appealing for applications in quantum information processing, magneto electric devices and next generation electronics/spintronics devices^{1,6–8}. Most of the earlier studies on TIs focus on their mysterious quantum transport properties^{1–8}. More recently however there has been a growing interest on their optical properties^{9–11}. In particular, related to their nano-structuring and the confinement effects, it has been proposed that three dimensional (3D) TIs such as Bi_2Te_3 , Bi_2Se_3 as well as two dimensional (2D) layered materials (MoS_2 , MoSe_2 etc.) could be the potential material for optical applications^{12–15}. Motivated by the interesting quantum properties of 3D TIs, in the present work, we focus on the photoluminescence (PL) studies of both bulk and mechanically exfoliated few layers of 3D TI Bi_2Te_3 single crystal. We observe a broad red emission in the visible region from 600 nm to 690 nm upon 375 nm excitation wavelength which corresponds to an optical band gap of 2 eV. In order to ensure the origin and confirmation of PL results, we have performed the PL measurements for both bulk and few layers (18 ± 2 nm) thin flakes of Bi_2Te_3 several times. This is in good agreement with our theoretical calculations. We have also explored in details about the topological surface states and possible inter band transitions of observed PL, using first-principles calculations. Our results show that Bi_2Te_3 as well other related TIs can act as ideal model systems for next generation optoelectronic device applications.

¹CSIR- National Physical Laboratory, Dr K S Krishnan Road, New Delhi, 110012, India. ²Academy of Scientific and Innovative Research (AcSIR), CSIR-National Physical Laboratory Campus, Dr K S Krishnan Road, New Delhi, 110012, India. ³Department of Physics and Astrophysics, Delhi University, New Delhi, 110007, India. ⁴Department of Physics, Indian Institute of Technology, Kanpur, U.P., 208016, India. ⁵Department of Physics, Banaras Hindu University, Varanasi, U.P., 221005, India. Correspondence and requests for materials should be addressed to B.K.G. (email: bipinbhu@yahoo.com) or V.P.S.A. (email: awana@nplindia.org)

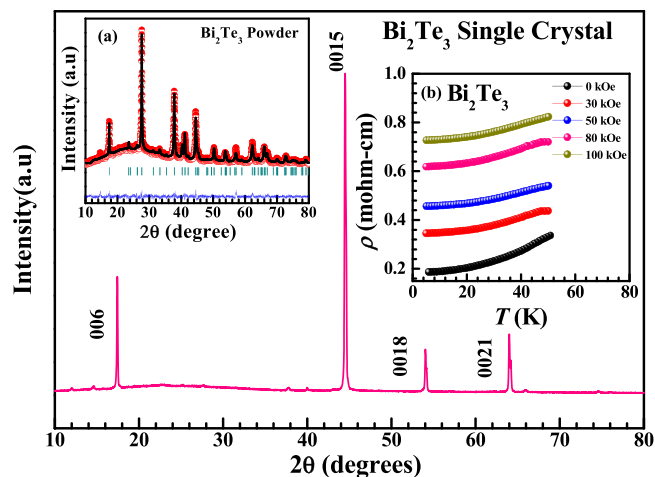


Figure 1. X-ray diffraction pattern for Bi_2Te_3 single crystal. Inset (a) shows the Rietveld fitted room temperature XRD pattern for powder Bi_2Te_3 crystal. (b) Temperature dependence of electrical resistivity at different magnetic fields for Bi_2Te_3 single crystal.

Results

Figure 1 shows the single crystal XRD pattern of bulk Bi_2Te_3 indicating that the crystal is highly textured i.e. c-axis oriented showing all the diffraction peaks corresponding to the (00l) reflections of the rhombohedral crystal structure with space group $R\bar{3}m(D_{3d}^5)$. The left inset of Fig. 1 represents the powder XRD pattern of bulk Bi_2Te_3 single crystal [Fig. 1(a)]. The lattice parameters found are $a = b = 4.3866(2) \text{ \AA}$ and $c = 30.4978(13) \text{ \AA}$. The right inset of Fig. 1 displays the temperature dependence of electrical resistivity at different applied magnetic fields for the synthesized Bi_2Te_3 single crystal having a temperature range of 5 K to 50 K [Fig. 1(b)]. The applied magnetic field varies from 0 kOe to 100 kOe. Here, the value of resistivity increases with increase in temperature from 5 K to 50 K representing metallic behavior with and without applied magnetic field. Thus, the nature of this plot is in agreement to that observed in our earlier reported studies¹⁶. The extensive ongoing research activity worldwide on TIs inspired us to further explore the PL properties of bulk and few layers of Bi_2Te_3 . As luminescent, insulators and semiconducting materials are widely studied, where PL originates from energy transfer from host to activator in the former and recombination of electron hole pair in the latter case. Energy transfer from insulators to conductors is also investigated in some composite systems^{17,18}. Apart from composites, there isn't any single material reported so far, where energy transfer from insulating to metallic states region takes place. It is well established that TIs are electronic materials having a bulk band gap like an ordinary insulator but have protected conducting states on their edges or surface. These states are protected by spin orbit interaction (SOI) and time reversal symmetry¹. These striking features of TIs make it more interesting to explore their optical behavior particularly photoluminescence nature. Previous studies on 3D TIs showed existence of dual band gaps; 0.3 eV corresponding to electronic band gap and 2.1 to 2.3 eV corresponding to optical band gap for the case of CVD grown Bi_2Se_3 nanoplatelets¹⁴. The existence of optical band gap in these materials give rise to a strong PL which we have investigated on the basis of experimental and theoretical calculations. It is well-known that Bi_2Te_3 has a layered crystal structure which consists of five atomic layers blocks, known as quintuple layer (QL)¹⁶. Each QL contains five atomic layers ordered as Te-Bi-Te-Bi-Te. The bonding inside a QL is strong ionic-covalent type whereas QLs are separated by weak van der Waals forces^{1,2,8}. The van der Waals gap in between the QLs makes Bi_2Te_3 cleavable as well as optically active.

The PL measurements are done for both bulk Bi_2Te_3 single crystal as well as for mechanically exfoliated few layers of Bi_2Te_3 . The optical images of both cases are shown in Fig. 2(a) and (b), respectively. The representative TEM images for bulk single crystal and few layers are shown in Fig. 2(c) and (d), respectively, which clearly differentiate between them. The SEM micrograph of Bi_2Te_3 as shown in Figure S1 (see Supplementary Information) clearly visualizes the layered structure. The TEM micrograph of bulk Bi_2Te_3 is shown in Figure S2 (see Supplementary Information) to further distinguish between bulk and exfoliated few layers Bi_2Te_3 . The decrease in transparency is associated with increase in number of QLs. Further, well resolved lattice fringes obtained from HRTEM micrograph in Figure S3 (see Supplementary Information) shows the formation of Bi_2Te_3 . The inter-planer spacing from the HRTEM micrograph comes out to be 0.21 nm. The SAED pattern with well indexed diffraction rings further confirms the lattice formation of Bi_2Te_3 as shown in Figure S4 (see Supplementary Information). Moreover, the atomic force microscopy (AFM) result confirms the thickness of mechanically exfoliated layers of Bi_2Te_3 is $(18 \pm 2) \text{ nm}$ as shown in Figure S5.

Angle resolved photoemission spectroscopy (ARPES) result shown in Figure S6 depicts energy distribution map (EDM) measured near the zone center for Bi_2Te_3 at a sample temperature of 20 K using 70 eV photon energy and p-polarized light. Dirac point is located at a binding energy of 300 meV below the Fermi level as shown by the green arrow on the EDM. The ARPES data is taken at Elettra synchrotron light source. This result clearly shows that the as synthesized Bi_2Te_3 single crystal is topological in nature because the band dispersion in the vicinity of the Fermi level as shown in Figure S6 is purely of the topological surface state (upper part of the Dirac cone)

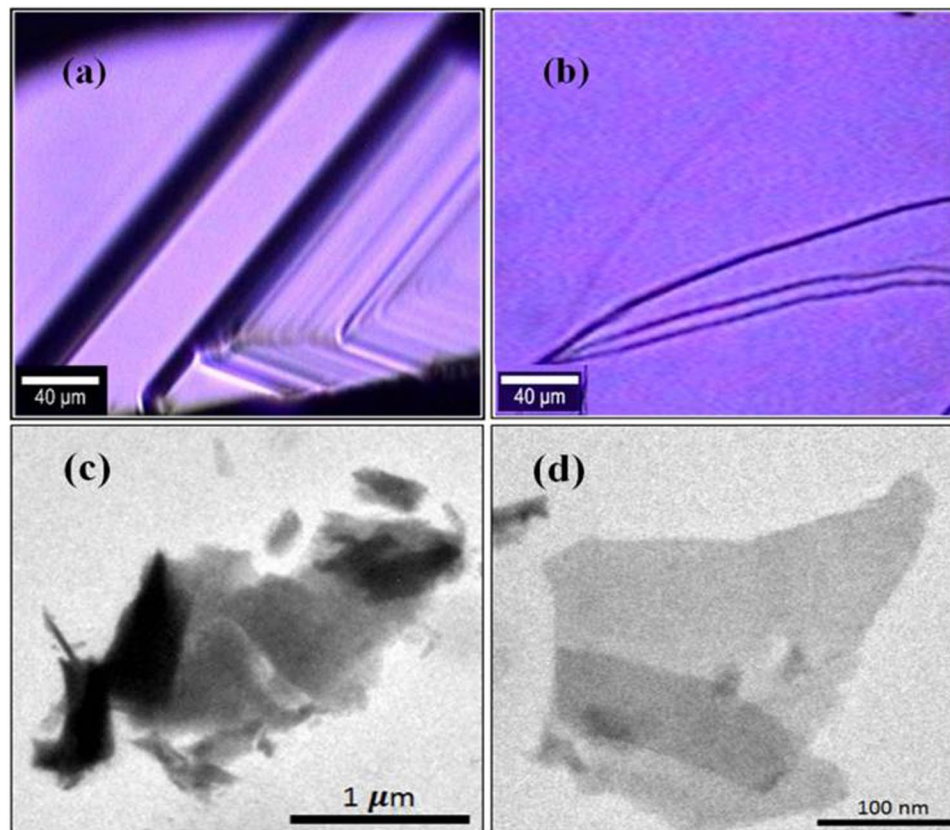


Figure 2. (a) Optical image of bulk Bi_2Te_3 single crystal. (b) Optical image of scotch tape taken from few layers of Bi_2Te_3 . (c) TEM image of bulk Bi_2Te_3 single crystal. (d) TEM image of few layers of Bi_2Te_3 .

although the Dirac point is at around 300 meV below the Fermi level. However, there are several reports discussing the presence of bulk bands near the Fermi level that are generally induced by the crystal disorder¹⁹. Thus, the absence of bulk bands near the Fermi level in our system suggests a high quality of the crystal with minimum defects. Figure 3(a) shows the PL emission spectra of both bulk Bi_2Te_3 single crystal and mechanically exfoliated few layers of Bi_2Te_3 upon excitation at 375 nm marked in black and red color respectively. The emission spectrum of bulk Bi_2Te_3 single crystal shows a strong red emission at 621.32 nm (~ 2 eV). Also, several other closely spaced spectral peaks appear in the red region from ~ 630 nm to 700 nm. Similar peaks were also observed in the case of mechanically exfoliated few layers of Bi_2Te_3 in the same region. However, significant enhancement in PL intensity is observed in the case of few layers of Bi_2Te_3 because of the decreasing number of QL which induces the efficient photon emission from few layers of Bi_2Te_3 due to internal transitions taking place in the sub-levels of this system. Accordingly, the optical penetration loss effect depends on the sample thickness. The present experimentally observed PL emission centered about 2 eV differs from that observed in the range of 2.1–2.3 eV for Bi_2Se_3 in another study¹⁴. The obvious reason could be the difference in two TI systems with different morphologies and dimensions having different inter band transitions which enable different optical band gaps.

The few layers of Bi_2Te_3 are mechanically exfoliated from the bulk single crystal using the standard scotch-tape method^{20–22} and hence, their thickness is considerably reduced to few QLs in comparison to the bulk Bi_2Te_3 single crystal where efficient photon emission is possible without the major peak shift like other 2D materials. In our investigated systems (Bi_2Te_3), we expostulate and understand the enhancement in PL emission is due to the higher photon emission into the thin flake of Bi_2Te_3 via Förster mechanism. More specifically, reduction of volume to surface area provides better photon energy emission due to internal transitions occurring in the sub-levels of the few layers of mechanically exfoliated Bi_2Te_3 without much of non-radiative loss like in the bulk system. Generally, PL may arise from such system due to defect or impurity present in crystal structure. The exact mechanism of the photon emission is however complex and requires further analysis. To further ensure the PL experiment and origin of PL, the absorbance analysis was performed to correlate with theoretical estimated data of mechanically exfoliated few layers of Bi_2Te_3 . The reflectance spectrum of mechanically exfoliated few layers of Bi_2Te_3 is shown in Figure S7 (see Supplementary Information). Figure 3(b) depicts the absorbance spectrum of mechanically exfoliated few layers of Bi_2Te_3 calculated using the formula $A = \log_{10} 1/R$, where A and R represents the absorbance and reflectance respectively. Here, we noticed strong absorption peaks at 576 nm and 663 nm which have good agreement with the observed PL peaks at 620 and 650 nm. Moreover, few more peaks are observed similar to the theoretical calculation of partial density of states (PDOS) [Fig. 4(a–b)]. In order to develop a better understanding of the underlying mechanism for observed PL, we employ density functional theory based calculations, using both the WIEN2k²³ as well as VASP²⁴ suite of codes. The generalized gradient

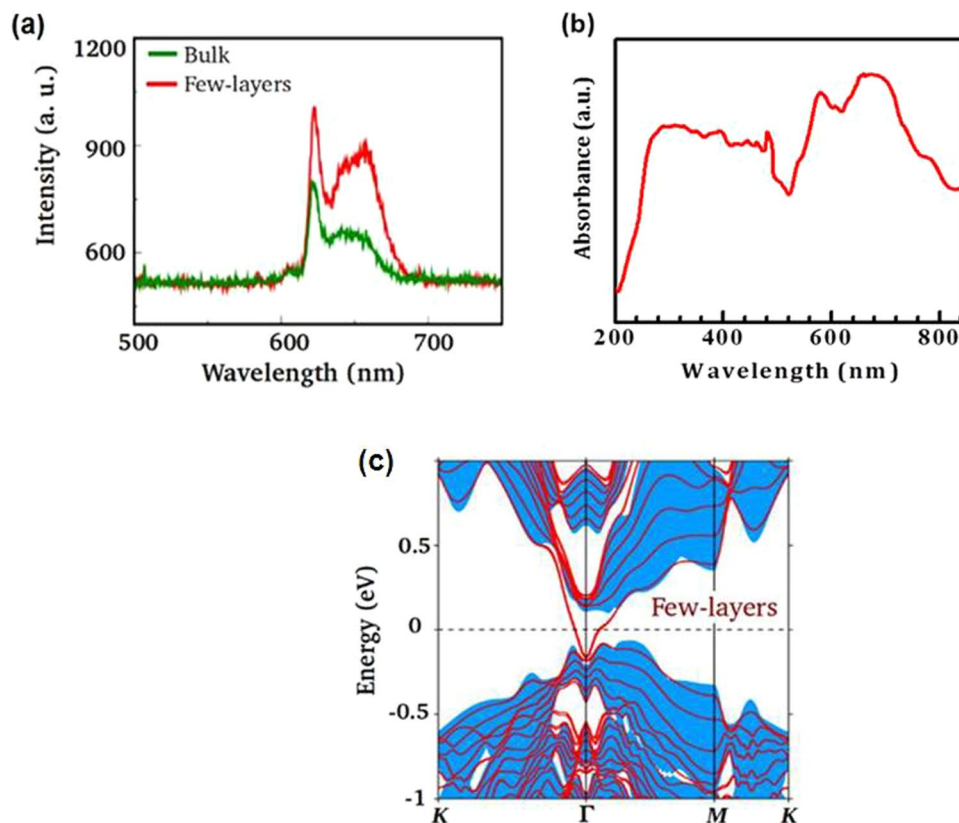


Figure 3. (a) PL spectrum of Bi_2Te_3 single crystal and mechanically exfoliated few layers. Green and red colors identify spectrum of bulk and few layers, respectively. (b) Absorbance spectrum of mechanically exfoliated few layers of Bi_2Te_3 . (c) A few layers band structure of Bi_2Te_3 with the inclusion of spin-orbit coupling along high symmetry directions in the (001) surface Brillion zone. Note that we have taken 6 QLs in our calculations as a representative case for few layers Bi_2Te_3 . The shaded part refers to the bulk states.

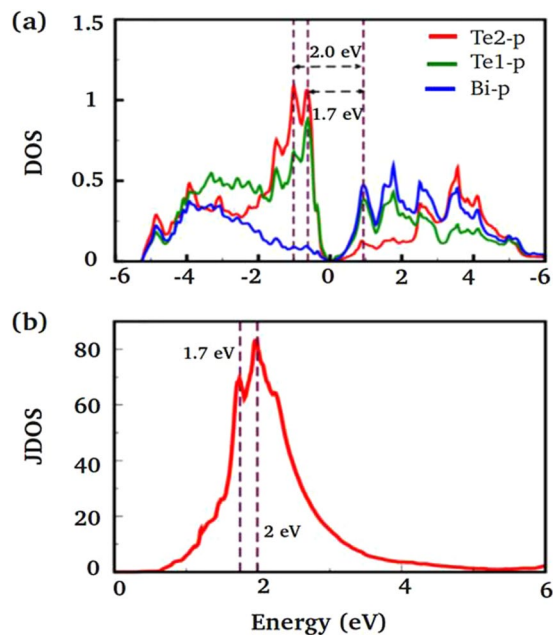


Figure 4. (a) Partial density of states (PDOS) and (b) Joint density of states (JDOS) for bulk Bi_2Te_3 with the inclusion of spin-orbit coupling. Te1 and Te2 in (a) represent Te atoms at the edge and the center of QL, respectively.

approximation (GGA) is used to include exchange correlation effects²⁵. Our calculations are performed with the inclusion of spin-orbit coupling (SOC). We have used 6 QLs to explicitly model few layers of Bi₂Te₃. The band structure of a few layers (6 QLs) of Bi₂Te₃ with the inclusion of SOC is displayed in Fig. 3(c) where the shaded part arises from the bulk. Our results show an insulating energy spectrum for bulk Bi₂Te₃ whereas its few layers have additional Dirac-cone-like conducting surface states inside the bulk energy gap. These results clearly demonstrate that Bi₂Te₃ is a topological insulator with different electronic states inside the bulk and on the surface and therefore, it is possible to have more photon emissions from such thin layers of Bi₂Te₃ due to the internal transitions of the sub-levels in the present TI system.

To further explore the energy levels electronic transitions responsible for PL emission, we show in Fig. 4(a-b) the partial density of states (PDOS) for bulk with the inclusion of SOC. It should be noted that PDOS of few layers of Bi₂Te₃ has significant change in comparison to the bulk, which is consistent with the experiments, except the appearance of small DOS at Fermi-level which is due to the presence of topological surface states. The PDOS profile clearly shows the existence of dominant electronic transitions between Te-p to Bi-p states. These electronic transitions have energies of ~1.7 eV and ~2 eV and are in substantial agreement with the observed PL peaks noted in Fig. 3(a). We have also found additional electronic transitions at higher energies and are not shown here as they lie away from the range of our measured PL spectra. Alternatively, we have calculated the joint density of states (JDOS) which does not have any broadening. The JDOS shown in Fig. 4(b) clearly identifies two dominant peaks at ~1.7 eV and ~2 eV, in qualitative agreement with our experimental observations except for the splitting size. This can be understood because of well known limitations of DFT in underestimating the gap. Hence a quantitative agreement with observed experimental is not possible.

Discussion

In conclusion, we report the optical band gap of bulk single crystals and mechanically exfoliated few layers of Bi₂Te₃ of around 2 eV, which is greater than its electronic band gap (~0.15 eV). This is consistent with our first-principles calculations. The experimentally observed 2 eV optical band gap in the visible region for bulk as well as for mechanically exfoliated few layers of Bi₂Te₃ clearly rules out the quantum confinement effects in the investigated samples which are the new paradigm shifts from other 2D systems like MoS₂, WS₂, WSe₂, MoSe₂, etc for 1–3 layers. Our results provide a stepping stone for further exploration of topological insulators for next generation optoelectronic, photonic, and spintronics applications.

Methods

The synthesis of bulk Bi₂Te₃ single crystal used for this study were carried out by self-flux method via the solid state reaction route¹⁶. High purity (99.999%) Bismuth (Bi) and Telluride (Te) powders were accurately weighed according to the stoichiometric ratio of 2:3 and mixed thoroughly using mortar and pestle inside a glove box filled with argon gas. The homogeneous mixture was then pressed into a rectangular pellet with the help of hydraulic press (40 kg/cm²) and vacuum sealed (10⁻³ Torr) in a quartz tube. Further, the quartz tube was kept inside a tube furnace and heated to 950 °C (2 °C/min) for 12 hours. The furnace was then allowed to cool very slowly to 650 °C (1 °C/30 min) after which it was switched off. The resultant crystal obtained was shiny and silver in color.

Measurements and Characterizations. In order to investigate the phase structure of the synthesized sample X-ray diffraction (XRD) was performed using Rigaku X-ray diffractometer with Cu-K α_1 radiation ($\lambda = 1.5418 \text{ \AA}$). The temperature dependent resistivity measurements were carried out using a quantum design 14 Tesla Physical Property Measurement System (PPMS). The thickness of the few layers of mechanically exfoliated Bi₂Te₃ was investigated by atomic force microscope (AFM, Model no. NT-MDT Solver Scanning probe Microscope). The absorbance measurements were carried out using Avantes spectrometer with AvaLight-DH-S-BAL balanced power source. For PL measurements, mechanically exfoliated^{20,21} few layers of Bi₂Te₃ were obtained using the standard scotch tape method²². However, the PL measurements were done using WITec alpha 300 R+ confocal PL microscope system using 375 nm diode laser as a source of excitation. In order to prevent the damage of bulk Bi₂Te₃ single crystal and few layers of Bi₂Te₃, caution was taken and the power setting for the excitation laser was maintained to lower values. Further, the surface morphology Transmission Electron Microscopy (TEM) was performed using Technai G20-twin operating at 200 kV. The ARPES data is taken at Elettra synchrotron light source at a sample temperature of 20 K using 70 eV photon energy and p-polarized light. In order to understand the measured PL spectrum we present density functional theory based calculations of the optical properties of Bi₂Te₃ for bulk and few layer structures.

References

- Hasan, M. Z. & Kane, C. L. Colloquium: Topological insulators. *Rev. Mod. Phys.* **82**, 3045–3067 (2010).
- Ando, Y. & Fu, L. Topological Crystalline Insulators and Topological Superconductors: From Concepts to Materials. *Annu. Rev. Condens. Matter Phys.* **6**, 361–381 (2015).
- Tang, H., Liang, D., Qiu, R. L. J. & Gao, X. P. A. Two-Dimensional Transport-Induced Linear Magneto-Resistance in Topological Insulator Bi₂Se₃ Nanoribbons. *ACS Nano* **5**, 7510–7516 (2011).
- Zhang, S. X. *et al.* Magneto-resistance up to 60 Tesla in topological insulator Bi₂Te₃ thinfilms. *Appl. Phys. Lett.* **101**, 202403–202406 (2012).
- Ning, W. *et al.* One-dimensional weak anti localization in single-crystal Bi₂Te₃ nanowires. *Sci. Rep.* **3**, 1564–1569 (2013).
- Fu, L., Kane, C. L. & Mele, E. J. Topological Insulators in Three Dimensions. *Phys. Rev. Lett.* **98**, 106803–106806 (2007).
- Moore, J. E. & Balents, L. Topological invariants of time-reversal-invariant band structures. *Phys. Rev. B* **75**, 121306–121309 (2007).
- Ando, Y. Topological Insulator Materials. *J. Phys. Soc. Jpn.* **82**, 102001–102032 (2013).
- Zhang, J. *et al.* Raman Spectroscopy of Few-Quintuple Layer Topological Insulator Bi₂Se₃ Nanoplatelets. *Nano Letters* **11**, 2407–2414 (2011).
- He, L. *et al.* Surface-Dominated Conduction in a 6 nm thick Bi₂Se₃ Thin Film. *Nano Lett.* **12**, 1486–1490 (2012).
- Wang, H. *et al.* Crossover between Weak Anti localization and Weak Localization of Bulk States in Ultrathin Bi₂Se₃ Films. *Sci. Rep.* **4**, 5817–5822 (2014).

12. Checkelsky, J. G., Hor, Y. S., Cava, R. J. & Ong, N. P. Bulk Band Gap and Surface State Conduction Observed in Voltage-Tuned Crystals of the Topological Insulator Bi₂Se₃. *Phys. Rev. Lett.* **106**, 196801–196804 (2011).
13. Zhao, M. *et al.* Actively Tunable Visible Surface Plasmons in Bi₂Te₃ and their Energy-Harvesting Applications. *Adv. Mater.* **28**, 3138–3144 (2016).
14. Vargas, A., Liu, F. & Kar, S. Giant enhancement of light emission from nanoscale Bi₂Se₃. *Appl. Phys. Lett.* **106**, 243107–243110 (2015).
15. Eda, G. *et al.* Photoluminescence from Chemically Exfoliated MoS₂. *Nano Lett.* **11**, 5111–5116 (2011).
16. Sultana, R., Neha, P., Goyal, R., Patnaik, S. & Awana, V. P. S. Unusual non saturating Giant Magneto-resistance in single crystalline Bi₂Te₃ topological insulator. *J. Magn. Mag. Mater.* **428**, 213–218 (2017).
17. Liu, X. & Lei, D. Y. Simultaneous excitation and emission enhancements in upconversion luminescence using plasmonic double-resonant gold nanorods. *Sci. Rep.* **5**, 15235–15246 (2015).
18. Fischer, S. *et al.* Plasmon enhanced upconversion luminescence near gold nanoparticles—simulation and analysis of the interactions. *Opt. Express* **20**, 271–282 (2012).
19. Chen, Y. L. *et al.* Experimental Realization of a Three Dimensional Topological Insulator, Bi₂Te₃. *Science* **325**, 178–181 (2009).
20. Cho, S., Butch, N. P., Paglione, J. & Fuhrer, M. S. Insulating Behavior in Ultrathin Bismuth Selenide Field Effect Transistors. *Nano Lett.* **11**, 1925–1927 (2011).
21. Hong, S. S. *et al.* Ultrathin Topological Insulator Bi₂Se₃ Nanoribbons Exfoliated by Atomic Force Microscopy. *Nano Lett.* **10**, 3118–3122 (2010).
22. Liao, Z. M. *et al.* Surface plasmon on topological insulator/dielectric interface enhanced ZnO ultraviolet photoluminescence. *AIP Advances* **2**, 022105 (2012).
23. Blaha, P., Schwarz, K., Madsen, G., Kvasnicka, D. & Luitz, J. WIEN2K, An Augmented Plane Wave + Local Orbitals Program for Calculating Crystal Properties K. Schwarz, Tech. Univ. Wien, Austria (2001).
24. Kresse, G. & Furthmüller, J. Efficient iterative schemes for ab initio total-energy calculations using a plane-wave basis set. *Phys. Rev. B* **54**, 11169–11186 (1996).
25. Perdew, J. P., Burke, K. & Ernzerhof, M. Generalized Gradient Approximation Made Simple. *Phys. Rev. Lett.* **77**, 3865–3868 (1996).

Acknowledgements

Authors from CSIR-NPL would like to thank their Director NPL India for his keen interest in the present work. This work is financially supported by DAE-SRC outstanding investigator award scheme on search for new superconductors. Rabia Sultana thanks CSIR, India for research fellowship and AcSIR-NPL for Ph.D. registration. SA would like to thank the High Performance Computing (HPC) facilities at Intra-University Accelerator Centre (IUAC) at New Delhi, Indian Institute of Mathematical Sciences (IMSC) at Chennai, CSIR- 4PI at Bengaluru, University of Hyderabad (UoH) in Hyderabad and Physics Department Indian Institute of Technology at Kanpur.

Author Contributions

B.K.G. and V.P.S.A. conceived the concepts of the research. R.S., G.A. and A.G. designed and synthesized the samples as well as performed the resistivity vs temperature measurements. S.S. performed the AFM and PL measurements of sample. A.K.S. performed the transmission electron microscopy of the sample. V.S., B.S. and S.A. performed the theoretical analysis. B.K.G., V.P.S.A., R.S., O.N.S. and S.A. wrote the manuscript and analysed the data.

Additional Information

Supplementary information accompanies this paper at <https://doi.org/10.1038/s41598-018-27549-0>.

Competing Interests: The authors declare no competing interests.

Publisher's note: Springer Nature remains neutral with regard to jurisdictional claims in published maps and institutional affiliations.



Open Access This article is licensed under a Creative Commons Attribution 4.0 International License, which permits use, sharing, adaptation, distribution and reproduction in any medium or format, as long as you give appropriate credit to the original author(s) and the source, provide a link to the Creative Commons license, and indicate if changes were made. The images or other third party material in this article are included in the article's Creative Commons license, unless indicated otherwise in a credit line to the material. If material is not included in the article's Creative Commons license and your intended use is not permitted by statutory regulation or exceeds the permitted use, you will need to obtain permission directly from the copyright holder. To view a copy of this license, visit <http://creativecommons.org/licenses/by/4.0/>.

© The Author(s) 2018